

Structure and Dynamics of Silica and Acrylamide Gels

Youngjun Song, Seung Soon Im,[†] Yang-Kyoo Han, and Daewon Sohn*

Department of Chemistry, Hanyang University, 17 Haengdang Dong, Seungdong Ku, Seoul 133-791, Korea

[†]Department of Textile and Polymer Engineering, Hanyang University, 17 Haengdang Dong, Seungdong Ku, Seoul 133-791, Korea

(Received December 21, 1999)

The structure and dynamics of silica and acrylamide gels were studied using a probe diffusion technique of dynamic light scattering (DLS). Latex particles, diameter = 0.05 μm , embedded in the gel network serve as a probe through their diffusion behavior within the network. A quantitative analysis of the homogeneity of the gel is introduced based on a shift of the correlation function of the dynamic light scattering. The lag time of the particles' correlation function in a completed inorganic silica gel is increased by increasing the contents of the gel network; but the particles' diffusion coefficient in a viscoelastic (acrylamide) gel lowers the $f(A)_{\text{max}}$, the maximum value of the y-axis in the correlation function. The silica gel makes a more homogeneous and compact structure than that of a PAA gel, which has partial heterodyning, by increasing the solid contents of the network density.

Silica gel is one of major precursors of aerogels, which are low-density porous solids; their excellent thermal insulation renders the material to be a good insulator. The insulation capability strongly depends on the porosity of the gel network, which is controlled by the chemistry of the precursor and the physics of the gelation process. The generally accepted gelation process is: 1) silica nanoparticles are generated at the beginning of the stage, 2) particles contact each other, 3) they then link to form bigger cluster networks. In any event, there exists a porous network, and the spacing of the network is a key factor in determining the thermal capability and color of the aerogel. X-Ray and electron microscopes are generally used to determine the structure of the gel network, though they simply provide local information about the gel structure. Dynamic light scattering (DLS) is a good candidate for pursuing both the gelation kinetics and the structure of a completed gel. Most DLS studies with gels had been based on a viscoelastic continuum picture of the gel network¹ until the non-ergodic framework² was developed. In a DLS experiment, the normalized time correlation function, $g^{(2)}(q, \tau)$, of the scattered intensity is given by

$$g^{(2)}(q, \tau) = \langle I(q, 0)I(q, \tau) \rangle / \langle I(q, 0) \rangle^2 \\ = 1 + f(A) |g^{(1)}(q, \tau)|^2, \quad (1)$$

where $f(A)$ is an instrumental coherence factor ranging from 0 to 1, which essentially gives the maximum ratio of the useful signal to the baseline; q is the magnitude of the scattering vector, $q = (4\pi n/\lambda) \sin(\theta/2)$, with n being the solution refractive index, θ the scattering angle, and λ the in vacuo wavelength of the incident light. For a monodispersed sample, $g^{(1)}(\tau) = \exp(-q^2 D \tau)$, where D is the translational diffusion coefficient. Although the angular brackets in Eq. 1 imply an ensemble average, they can be replaced by a time

average based on ergodicity theorem in most DLS experiments. In a gel, the total scattered field may be written² as the sum of the fluctuating component, $E_F(q, t)$, and a time-independent component $E_c(q)$, $E(q, t) = E_F(q, t) + E_c(q)$. The time-average of the total scattered intensity can be expressed as $\langle I(q) \rangle_T = \langle |E(q, \tau)|^2 \rangle_T = \langle I_F(q) \rangle_T + I_c(q)$, where $\langle I(q) \rangle_T$, $\langle I_F(q) \rangle_T$, and $I_c(q)$ indicate the correlation function of the total scattered intensity, the fluctuating component, and the time-independent component, respectively. The time-average intensity correlation function is a mixture of a Gaussian and a constant field having a homodyne contribution and a heterodyne part of the total intensity correlation. The diffusion of the probe particles in porous medium³ depends on the diameter of the probe, d , and the correlation length, ξ , of the network. Thus, the structure and morphology of the gel can be explained by characterizing the probe particle in a polymer gel.^{4–6}

An aim of this study was to investigate the porosity and structure of the silica gel by using dynamic light scattering with standard latex particles. The homodyne and the heterodyne contributions to the probe diffusion of normal latex particles in the gel were investigated using polarizing light scattering; their heterogeneities were compared with a viscoelastic polyacrylamide gel. The shift of $f_{\text{max}}(A)$ and the lag time of the correlation function represent the coherence length of the gel network and the structural characteristics of two different gels. Quantitative information concerning the homogeneity of the gel was introduced based on the shift of the correlation function of the dynamic light scattering.

Experimental

The silica-gel^{7–10} preparation consists of two steps: a) the preparation of a sol-gel stock solution by acid-catalyzed esterification; and b) gelation by basic catalysis and aging (polycondensation). To

make a stock solution, 30 ml of tetraethyl orthosilicate (TEOS), 30 ml of ethanol, and 2.5 ml of deionized water were mixed in a round-bottom flask. As a catalyst, 0.1 ml of 1 M ($1 \text{ M} = 1 \text{ mol dm}^{-3}$) HCl was added. The molar ratios among the TEOS, EtOH, and water were adjusted depending on the desired correlation length and the reaction time. The mixed solution was stirred for 1.5 h. at 60°C . The sample was then cooled down to room temperature. This was the precursor (stock solution) for the silica gel. In the next step, 0.2 ml 0.1 M aq NH_3 was added to 2 ml of the stock solution, followed by filtration with a $0.1 \mu\text{m}$ Millipore Millex-VV filter in a cylindrical light-scattering cell. The gelation time was varied by the ratio of TEOS/EtOH/ H_2O and mostly by the amount of the added base. The typical gelation time was 15 min to 3 h. Different molar ratios of TEOS/EtOH had been made by the same method. A solution 0.05 ml containing latex particles was added to the pregel mixture prior to initiation of the gelation by an aqueous ammonia catalyst. The cells were flushed with argon and sealed.

Polyacrylamide gels¹¹ or solutions were made by copolymerizing acrylamide (AA, Aldrich) and *N,N'*-methylenebisacrylamide (BAA, Aldrich) using ammonium peroxosulfate (AP) as an initiator and *N,N,N',N'*-tetramethylethylenediamine, (TEMED, Aldrich, 99%) as the activator. In 10 ml of clean water, 0.01 g (6.48×10^{-3} mol) of BAA and 0.24 g (0.34 mol) of AA were dissolved. This was a stock solution of 2.5 wt% and 4% BAA/AA ratio. Various concentrations and BAA/AA ratio (1–40%) stock solutions were made by the same method. The stock solution was dedusted using a $0.1 \mu\text{m}$ Millipore VV-type filter. A stock solution (1 ml) was placed into the LS cell, and a 2.5% 0.05 ml solution containing normal latex particles was added. The final latex concentration was 0.13%. 3 μl of TEMED (Aldrich, 99%) and 5 μl of 0.5 M ammonium peroxosulfate were added to initiate gelation. They were flushed with argon and sealed.

The probe particles used in this experiment were commonly available small and uniform (diameter ca. $0.05 \pm 0.01 \mu\text{m}$) latex particles. Particles were purchased from Polysciences, 2.5 wt% of solutions, which have sulfonated charges on the surface. A solution containing latex particles was filtered with a $0.1 \mu\text{m}$ Millipore filter before mixing with the gel precursor.

The light-scattering instrument¹² consisted of a He–Ne laser of 632.8 nm for polarized measurements. Because the laser beam was approximately vertically polarized, a low-power Glane–Thomson polarizer was sufficient to eliminate the small horizontal component. An EMI 9863 photomultiplier tube was connected to a Pacific Precision Instrument (Model AD 126) photon counting system. An ALV-5000 digital autocorrelator was used to measure the correlation function with multiple runs to approach the gelation process. The sample was held inside a refractive-index matching toluene bath. The temperature was controlled to $25 \pm 0.1^\circ\text{C}$ by nonturbulent water circulation through a pure copper block. The position of the sample was changed by connecting to a stepping motor to average the autocorrelation functions, (at least 50 different spots).

Results and Discussion

To monitor the kinetic growth of the silica cluster, DLS was used to determine the diffusion coefficients and hydrodynamic radii. Figure 1 shows the time-dependent hydrodynamic radii (a), and the diffusion coefficients (b) during the gelation of silica gel without any probe particles. The sample has 0.5 ml TEOS and 10 ml EtOH, catalyzed with aq NH_3 . We collected autocorrelation functions every 2 min, and each sample time was 20 s, respectively. The diffusion coeffi-

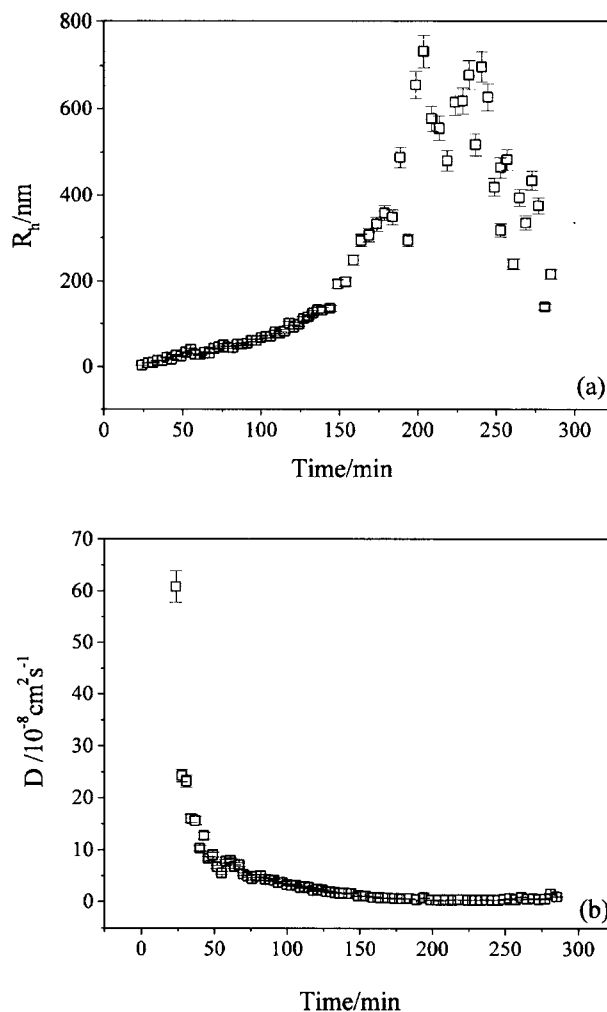


Fig. 1. (a) Hydrodynamic radius change of the silica sol-gel transition with time, $R_h = kT/6\pi\eta D$. Sample composition was 0.5 ml TEOS, 10 ml EtOH, catalyzed with NH_4OH . Light scattering measurement was done at 25°C , 90° scattering angle. (b) Diffusion coefficient is from the 3rd cumulant of the ALV correlator, (3–128 channels).

cients and hydrodynamic radii were deduced from the 3rd cumulant fitting of the autocorrelation functions in 3–128 channels and the Stokes–Einstein equation, $D = kT/6\pi\eta R_h$. The size of the particles was abruptly increased at the beginning of the gelation process, which in this experiment was faster than the diffusion-limited aggregation; t_{gel} = less than 3 h.^{13,14} After the gelation process was completed, the viscosity of the gel rose abruptly, and a near-perfect plasticity or linear-hardening¹⁵ behavior was observed. DLS experiments showed no correlation after the gelation process was completed.

When we inserted polystyrene latex particles to the sol of the silica precursor, the scattered intensity of the latex particles was much larger than that of growing clusters. Because there is competition between the latex particles and growing clusters, it is too hard to separate the decay rate of each different species during the gelation process. However, the latex particles' decay is evident in the completed gel

structure, which has no correlation of the gel network, itself. The intensity ratio ($I_{\text{latex in gel}}/I_{\text{gel}} \approx 3$) between latex particles and the gel network has been averaged because of the non-ergodic properties of the gel. The apparent diffusion coefficient of the latex particle is $3.0 \times 10^{-8} \text{ cm}^2/\text{s}$ in the initial sol state, turning to $2.7 \times 10^{-8} \text{ cm}^2 \text{ s}^{-1}$ in the completed gel of 0.01 M ratio of TEOS/EtOH. Figure 2 shows the correlation function of the latex particles in the gel, and compares it with that of latex particles in water. Even though the diffusion coefficient slows down, $D = 7.74 \times 10^{-8} \text{ cm}^2 \text{ s}^{-1}$ in water and $D \approx 3.0 \times 10^{-8} \text{ cm}^2 \text{ s}^{-1}$ in the gel structure, latex particles move freely inside of the pores, which implies that the mesh size is bigger than the particle diameter. The initial decays of the correlation functions in Fig. 2 were chosen to deduce the diffusion coefficients.

When we changed the molar ratio of TEOS/EtOH (0.013, 0.025, 0.030, 0.037, 0.045), corresponding to the volume percentages of TEOS (5, 10, 12, 15, 20%), the diffusion coefficients of the latex particles slowed down linearly. The high molar ratio of TEOS/EtOH gel does not show particle diffusion when the length scale of the light scattering, $2\pi/q$, is 450 nm, and the low molar ratio solution (< 0.013) does not form a gel, even after 1 month. Figure 3 shows the correlation function of 0.059 μm sulfonated latex particles in different TEOS/EtOH ratios of the completed silica gel. Each correlation function is averaged from more than 50 different spots of the gel by rotating the sample using a computer-driven stepping motor. The measurements were

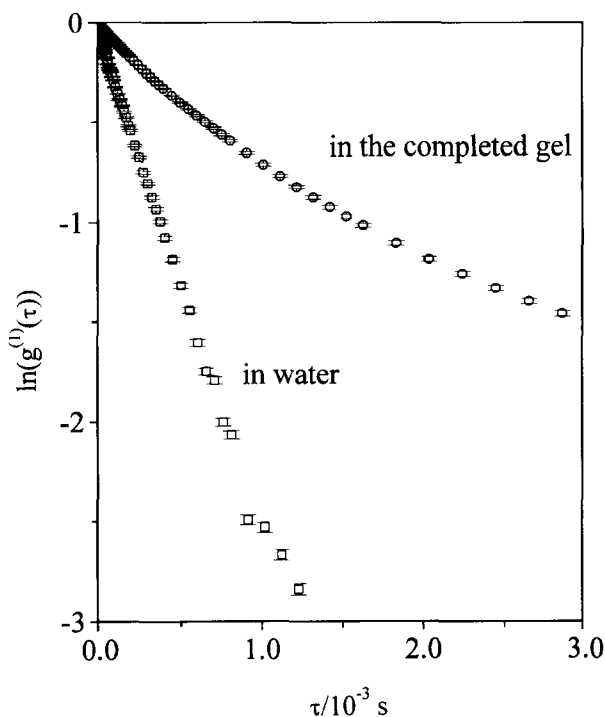


Fig. 2. Correlation function of polystyrene latex particles, diameter = 0.059 μm , in the silica gel network, compared to that in the water. The composition of the gel is 0.5 ml TEOS, 10 ml EtOH, catalysed with NH_4OH . Measurement was performed at 25 $^\circ\text{C}$, 90 $^\circ$ scattering angle.

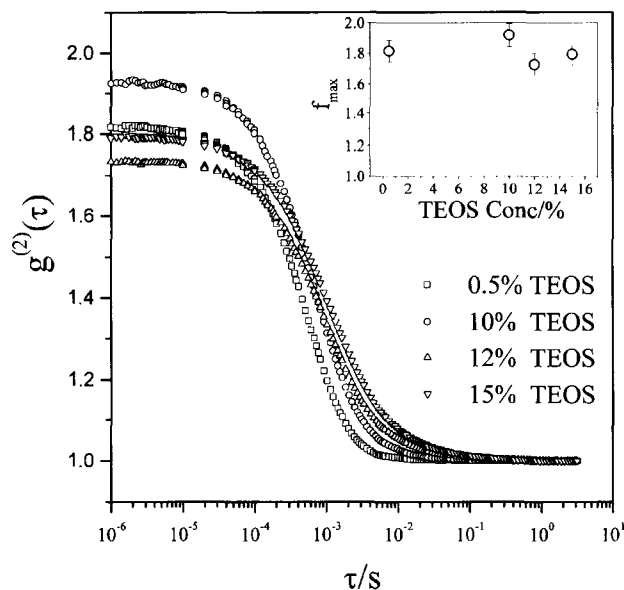


Fig. 3. Correlation function of the latex particles, diameter = 0.059 μm , in different TEOS/EtOH ratio of completed silica gel. TEOS/EtOH molar ratios are 0.013, 0.025, 0.030, and 0.037, respectively. Each correlation function is averaged from more than 50 different spots of the gel. Measurement is performed with 632.8 nm He-Ne laser at 25 $^\circ\text{C}$, 90 $^\circ$ scattering angle. The insert is the plot of f_{max} , the maximum value of the y axis in the correlation function, vs. TEOS concentration (%).

performed with a 632.8 nm He-Ne laser at 90 $^\circ$ angle and 25 $^\circ\text{C}$. The diffusion coefficient of latex particles in water, D_0 , $7.74 \times 10^{-8} \text{ cm}^2 \text{ s}^{-1}$, is higher than that with the lowest TEOS/EtOH ratio silica solution.

Figure 4 shows that the diffusion coefficient of latex particles in the completed silica gel decreases by increasing the TEOS/EtOH molar ratio. The relative diffusion coefficients compared with the particle diffusion in water, $D_0 = 7.74 \times 10^{-8} \text{ cm}^2 \text{ s}^{-1}$, are indicated.

The corresponding correlation length, ξ , of the gel is indicated in the upper x-axis of the plot, which is deduced based on the experimental data. The particles' relative diffusion coefficients varied linearly with the gel correlation length. Several different groups have observed the linear relation of D/D_0 against ξ , which was summarized by Muhr and Blanshard.¹⁶ We postulated that the correlation length of the completed gel, where no motion of at 0.058 M ratio, is the same as the size of the particle, 0.059 μm . Another length scale deduced from the plot is the average distance of a particle in the solution, 0.37 μm . It should be the length scale at 0 molar ratio of TEOS/EtOH, which is estimated using the relation $v \xi^3 = 1$, where v is the number density and ξ is the correlation length. There is a linear relation between the correlation length and the diffusion coefficient. The linear relation of the correlation in Fig. 4 means that the gel structure shrinks more uniformly than that of the PAA gel, is discussed in the next section. Most of the correlation signal comes from the fluctuating part of the gel/particle ternary structure, not from the gel structure. Non-ergodic

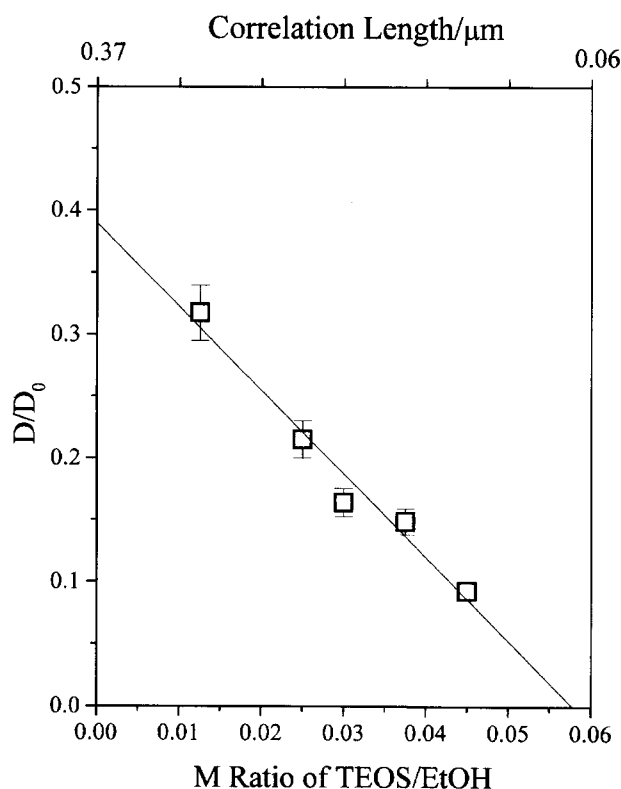


Fig. 4. Diffusion coefficient of latex particles in the completed silica gel decreased by increasing the TEOS/EtOH molar ratio. $D_0 = 7.74 \times 10^{-8}$ cm²/s. The corresponding correlation length, ξ , of the gel is indicated in the upper x-axis in the plot.

considerations of the intensity correlation function explain a small shift in the baseline, but no dramatic shift in $g^{(2)}(\tau)$. The shift of the $g^{(2)}(\tau)$ in this ternary system can show the trapping of particles in the gel structure. A complex dynamical behavior ranging from the purely *translational diffusion* of latex particles in the medium to a *relaxational* (slowing down) *behavior* associated with a local movement of probes in the gel has been discussed by a couple of groups.^{17–20} An idea of Pusey and van Megen,² who proposed a non-ergodic concept for a speckle pattern of the gel composed of both fluctuating and non-fluctuating components, cannot apply to silica gel, because the gel has a uniform scattering signal, $g^{(2)}(\tau)$, in the scattering volume. On the other hand, a viscoelastic gel, like polyacrylamide, has totally different intensity autocorrelation functions. PAA gel becomes too turbid to allow a measurement of the scattered intensity when the (BAA+AA)/water ratio is over 5 wt% and the (BAA/AA) ratio is over 20%. We used a V_v (vertically polarized incident beam and vertically detected beam) measurement before the onset of turbidity. The particles' autocorrelation function from the polarized light scattering in 3 different concentrations (2.5, 3.5, 4.5% PAA) of completed PAA gel (BAA/AA = 0.04) is shown in Fig. 5.

Each correlation function is the average of more than 50 different intensity correlation functions of different speckle patterns. We collected the scattering signal during a 60 s

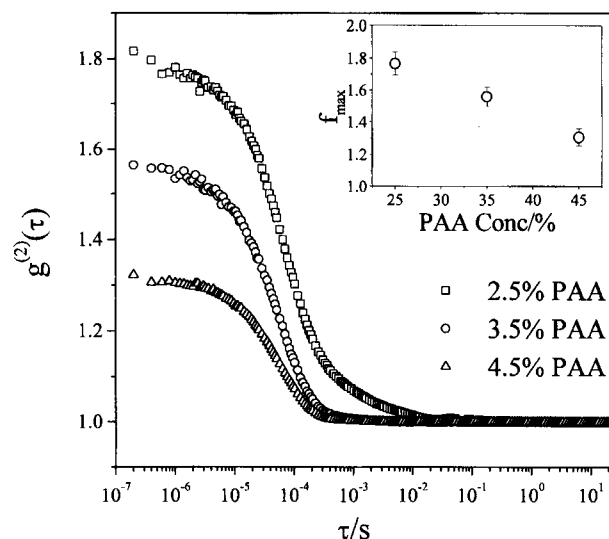


Fig. 5. The time averaged autocorrelation function of the particles in 3 different concentrations (2.5, 3.5, and 4.5 wt%) of PAA gel from the 50 different spots. The measurement was performed with 632.8 nm He–Ne laser, 600/50 pin-hole setting at 25 °C, 90° scattering angle. The insert is the plot of f_{\max} , the maximum value of the y axis in the correlation function, vs. PAA concentration (%).

sample time for each speckle pattern, which was sufficient to obtain a reasonably smooth intensity correlation function; also, the correlation function is not shifted from the baseline. Then, each time correlation function was summed, and 50 correlation functions were averaged using the QUICK BASIC program. From the averaged time-correlation function, which is not the ensemble average, one feature is obvious from a plot of PAA gel: $f(A)_{\max}$: the maximum value of the y-axis in the correlation function decreases with increasing gel concentration (wt% of BAA+AA), which indicates partial heterogeneity due to the emergence of strongly scattered particles and stationary clusters of the gel. Generally, although a non-ergodic medium has a baseline shift of $g^{(2)}(t)$ during the process of ensemble averaging, there was no dramatic difference between the time- and ensemble-averaged autocorrelation functions in the particle-gel system. Joosten et al.⁷ reported that the intensity autocorrelation function of polyacrylamide gel, obtained from a dynamic light-scattering experiment, is not equal to the ensemble-averaged correlation function. The major difference between these two systems is the presence of particles in the gel, which generate particle diffusion inside of the completed gel associated with the fluctuating component of the intensity autocorrelation function. The autocorrelation function of the polyacrylamide gel/particle system is totally different from the silica gel/particles behavior. By decreasing the correlation length, ξ , the diffusion coefficient is decreased and the correlation function is shifted to a short time scale in the case of the silica gel, but the $f(A)_{\max} = g^{(2)}(q, t) - 1/g^{(1)}(q, t)^2$, shifts to lower values in the polyacrylamide gel. It is clear that trapped particles act as local oscillators which cause partial heterodyning in the acrylamide gel, and lower the value of $f(A)_{\max}$. The

$f(A)_{\max}$ values reflect the coherence of the scattering signal related to the coherence area. The view volume includes more non-fluctuating gel components with an increase of the gel concentration accompanied by a decreased contribution of the scattering from particles. The ratio between the fluctuating and stationary component in Fig. 5 is 0.81, 0.47, and 0.20 for 2.5, 3.5, and 4.5% PAA gel, respectively. Low $f(A)_{\max}$ values may indicate partial heterodyning due to the emergence of stationary structures. In the PAA gel, the finite value of $f(A)_{\max}$ is endowed with fluctuating and stationary components, which come from the diffusion of the particles in the gel and the gel heterogeneity, respectively. The insert of the graph emphasizes the difference of $f(A)_{\max}$ between the polyacrylamide gel and the silica gel. The silica gel originating from interconnected colloidal particles is macroscopically more homogeneous than the viscoelastic PAA gel. The shift in the particles' diffusion coefficients in silica gel comes from the homogeneity of the solid silica-gel network. And the $f(A)_{\max}$ lowering of the correlation function for the particles in the acrylamide gel comes from the viscoelastic property of the heterogeneous gel structure. Probe-diffusion studies of particles in gels give an idea about the porosity of the gel, the correlation length in the gel network and the homogeneity of the gel structure.

Probe diffusion with latex particles in two different types of chemically cross-linked gels, silica gel and acrylamide gel, has been studied by dynamic light scattering. The diffusion coefficients of particles in completed inorganic silica gel are decreased by reducing the gel correlation length; on the other hand, the particles' diffusion coefficients in a viscoelastic (acrylamide) gel lower the $f(A)_{\max}$. By increasing the contents of the gel network, the silica gel makes a more homogeneous and compact structure than that of the PAA gel, which has partial heterodyning. The structural difference between these two gels comes from the origin of the gelation process; the silica gel is made from the physical aggregation of small particles, but the acrylamide gel is generated from a continuous chemical bond.

D. S. is indebted to Prof. P. S. Russo of the department of chemistry at Louisiana State University for his valuable com-

ments. This work was supported by the Research Institute of Natural Science at Hanyang University and partially by the Ministry of Education in 1998.

References

- 1 T. Tanaka, L. O. Hocker, and G. B. Benedek, *J. Chem Phys.*, **59**, 5151 (1973).
- 2 P. N. Pusey and W. van Megen, *Physica A*, **157**, 705 (1989).
- 3 R. J. Berne and R. Pecora, "Dynamic Light Scattering with Applications to Chemistry, Biology and Physics," Wiley, New York (1976).
- 4 G. J. M. K. Sebastiaan, J. K. G. Dhont, and A. P. Philipse, *Langmuir*, **13**, 4982 (1997).
- 5 C. Allain, M. Drifford, and B. G.-Manuel, *Polym. Commun.*, **27**, 177 (1986).
- 6 C. Konak, R. Bansil, and J. C. Reina, *Polymer*, **31**, 2333 (1990).
- 7 J. G. H. Joosten, E. T. F. Gelade, and P. N. Pusey, *Phys. Rev. A*, **42**, 2161 (1990).
- 8 C. J. Brinker and G. W. Scherer, "Sol-Gel Science," Academic Press, San Diego (1990).
- 9 H. D. Gesser and C. Goswami, *Chem. Rev.*, **89**, 765 (1989).
- 10 D. W. Schaefer, B. J. Oliver, C. S. Ashley, D. Richter, B. Farago, B. Frick, L. Hrubesh, M. J. van Bommel, G. Long, and S. Krueger, *J. Non-Cryst. Solids*, **145**, 105 (1992).
- 11 J. Baselga, I. H. Fuentes, I. F. Pierola, and M. A. Llorente, *Macromolecules*, **20**, 3060 (1987).
- 12 D. Sohn, P. S. Russo, D. B. Roitman, *Ber. Bunsenges. Phys. Chem.*, **100**, 821 (1996).
- 13 J. E. Martin and J. P. Wilcoxon, *Phys. Rev. A*, **39**, 252 (1988).
- 14 J. E. Martin and J. P. Wilcoxon, *Phys. Rev. Lett.*, **61**, 373 (1988).
- 15 T. Tanaka, "Encyclopedia of Polymer Science and Engineering," 2nd ed, ed by H. F. Mark et al., Wiley, New York (1986), Vol. 7, p. 514.
- 16 A. H. Muhr and J. M. V. Blanshard, *Polymer*, **23**, 1012 (1982).
- 17 I. Nishio, J. C. Reina, and R. Bansil, *Phys. Rev. Lett.*, **59**, 684 (1987).
- 18 S. Pajevic, R. Bansil, and C. Konak, *Macromolecules*, **26**, 305 (1993).
- 19 L. Fang and W. Brown, *Macromolecules*, **25**, 6897 (1992).
- 20 B. Camins and P. S. Russo, *Langmuir*, **10**, 4053 (1994).